

Synthesis and characterization of Gd doped **La_2NiMnO_6**

A THESIS SUBMITTED IN PARTIAL FULFILMENT OF THE REQUIREMENTS FOR
THE DEGREE OF

Master of Science in Physics



By

Sushree Sangita Naik

Roll No. – 412PH2105

Under the supervision of

Dr. Prakash Nath Vishwakarma

DEPARTMENT OF PHYSICS
NATIONAL INSTITUTE OF TECHNOLOGY, ROURKELA
2012-2014



CERTIFICATE

This is to certify that the thesis entitled “**Synthesis and characterization of Gd doped $\text{La}_2\text{NiMnO}_6$** ” submitted by Miss. Sushree Sangita Naik in partial fulfillment of the requirements for the award of master of science degree in physics at National Institute of Technology, Rourkela, is an authentic work carried out by her under my supervision and guidance.

To the best of my knowledge, the matter embodied in the thesis has not been submitted to any other organization.

Date:

Prof. Prakash N. Vishwakarma
Dept. of Physics
National Institute of Technology,
Rourkela – 769008

ACKNOWLEDGEMENTS

On the submission of my thesis “*Synthesis and characterization of Gd doped $\text{La}_2\text{NiMnO}_6$* ”, I would like to convey my gratitude to my supervisor Prof. Prakash Nath Vishwakarma, Department of Physics for his constant support and guidance during the course of my work in the last one year. I appreciate and value his esteemed guidance and encouragement from the beginning to the end of this thesis. I am indebted to him for having helped me shape the problem and providing insights towards the solution.

I am thankful whole heartedly to Mr. Achyuta Kumar Biswal, PhD scholar, Department of Physics for steadily helping us in our project work without any hesitancy. I am obligated to him for helping in every respect with utmost patience. Also I am thankful to Miss Jashashree Ray, PhD scholar, Department of Physics for giving moral support and valuable suggestions and helping us in project work. I am also thankful to Mr. Sourav Kuila, PhD scholar for helping me when I'm in need.

I thank my lab-mate Miss Shyama Mohanty for accompanying me throughout the year and giving me strength and confidence to complete the project successfully. I also thank Mr. Debi Prasad Pattanaik for his constant moral support and necessary help.

I am grateful to the institute, National Institute of Technology Rourkela for providing a very good laboratory facility.

Above all, I would like to thank all my friends whose direct and indirect support helped me completing my project in time. This thesis would have been impossible without their perpetual moral support.

Sushree Sangita Naik

CONTENTS

Chapter 1

Introduction

I. Recent research on oxides

I.1 Superconducting Oxides

I.2 Ferroelectric Oxides

I.3 Magnetic Oxides

I.4 Multiferroic Oxides

II. Multiferroics

Primary Ferroic order parameter

III. Perovskites

III.1 Double Perovskites

III.2 About $\text{La}_2\text{NiMnO}_6$

Chapter 2

Literature Survey

Chapter 3

Experimental

I. Synthesis

II. Flow chart

Chapter 4

Results and discussion

I. XRD analysis

II. DC Resistivity measurement

III. Dielectric Measurement

Chapter 5

CONCLUSION

REFERENCES

ABSTRACT

Multiferroic $\text{La}_2\text{NiMnO}_6$ and the Gd doped $(\text{La}_{1-x}\text{Gd}_x)_2\text{NiMnO}_6$, ($x=0, 0.1$ & 0.2) samples are prepared by sol - gel technique by using citric acid and ethylene glycol. X-ray diffraction confirms the phase purity of $(\text{La}_{1-x}\text{Gd}_x)_2\text{NiMnO}_6$ ($x=0, 0.1$ & 0.2) as well as the crystal structure. All the samples are crystallized in monoclinic structure with space group $\text{P}2_1/\text{n}$. The electrical transport measurement is carried out for $(\text{La}_{1-x}\text{Gd}_x)_2\text{NiMnO}_6$, ($x=0, 0.1$ & 0.2) by two probe method and as a result the enhancement of insulating behavior with Gd concentration at room temperature is obtained. In addition to this the thermally activated behavior is observed for all the three samples and the activation energy decreases with the increase in temperature. Temperature dependent dielectric measurement all the samples in the frequency range 100 Hz to 100KHz shows step like decrease in dielectric constant, and loss tangent show corresponding relaxation peak. With increase in Gd – substitution, non-dispersive region of dielectric is shifted to high temperature. The relaxation peak in the loss spectra also shifts to higher temperature with Gd – substitution. Room temperature dielectric loss vs frequency spectra show with Gd - substitution loss decreases.

CHAPTER 1

I. **RECENT RESEARCH ON OXIDES:-**

From the very beginning of condensed matter research, oxides have earned a considerable interest for their wide device applications as well as underlying fundamental physics. Research on oxide includes spectacular phenomena like superconductivity, ferroelectricity, magnetism and multiferroicity etc. Low cost and less sophisticated processing condition makes them unique from metals and pure semiconductors. Oxides of different forms like Single crystals, polycrystalline powder, and thin films are used in various potential applications such as transducers, power electronics, memory devices, sensors and actuators etc. [1]

I.1 Superconducting Oxides:-

Dutch physicist K. Onnes first discovered superconductivity in mercury in 1911 in Leiden University. A lot of researches have been carried out that day onwards on variety of sample. [2] The main aim of the researchers is to bring its critical temperature towards room temperature for various device applications. The high temperature superconductors were discovered, whose superconducting transition temperature was much above that predicted by BCS theory for conventional superconductors. Some of the high temperature superconductors are listed as below. [3]

1.2 Ferroelectric Oxides:-

Ferroelectricity is a property of certain materials that have a spontaneous electric polarization. Ferroelectricity arises due to their displacive (such as BaTiO_3) or order-disorder (such as NaNO_2) transition. In ferroelectric oxides, the order parameter can be understood in terms of a polarization catastrophe, in which, if an ion is displaced from equilibrium position slightly, the force from the local electric fields due to the ions in the crystal increases very rapidly than the elastic-restoring forces. [4] This results in an asymmetrical shift in the equilibrium ion positions and hence gives a permanent dipole moment. For example: the ionic displacement in barium titanate gives the relative position of the titanium ion within the oxygen octahedral cage. The spontaneous polarization of ferroelectric materials gives a hysteresis effect which can be used as a memory devices, and ferroelectric capacitors are indeed used to make ferroelectric RAM. [5]

Table 2

Material	Dielectric constant
CaTiO_3	300
SrTiO_3	310
BaTiO_3	1250-10,000

I.3 Magnetic Oxides:-

Oxides of transition metals are the most explored magnetic nanoparticles up to date. The magnetic oxides are the everlasting research topics because of their wide applications. The nanoform of magnetic oxides sometime exhibit superparamagnetic behaviour which prevents self-agglomeration among the particles and the magnetic behavior arises only when an external magnetic field is applied. [7] The remanence magnetization disappears with the removal of the magnetic field. Iron oxides are the most promising candidate as they have variety applications such as soft magnet and hard magnet. The overwhelming application of iron (III) oxide is as the feedstock of the steel and iron industries, e.g. the production of iron, steel, and many alloys. [6]

Table 3

Material	Magnetic flux density (Tesla) at room temperature	Ferromagnetic Curie temperature(T_c) in K
NiFe₂O₄	270	860
CoFe₂O₄	480	790
MnFe₂O₄	400	570

1.4 Multiferroic Oxides:-

Materials having more than one ferroic order parameter (ferroelectricity, ferro/antiferromagnetic, ferroelasticity) are considered as multiferroics. The existence of coupling of various order parameters renders it for various applications such as transducers, memory devices etc. [8] Due to presence of both ferromagnetism and ferroelectricity in the same material, it exhibits ferromagnetic & ferroelectric properties or there exist a coupling of these two properties in a single material as well as in compound. Since its discovery, a lot of research is going on to discover various multiferroic oxides e.g. BiFeO_3 , YMnO_3 , TbMnO_3 , LuFe_2O_4 etc. [9]

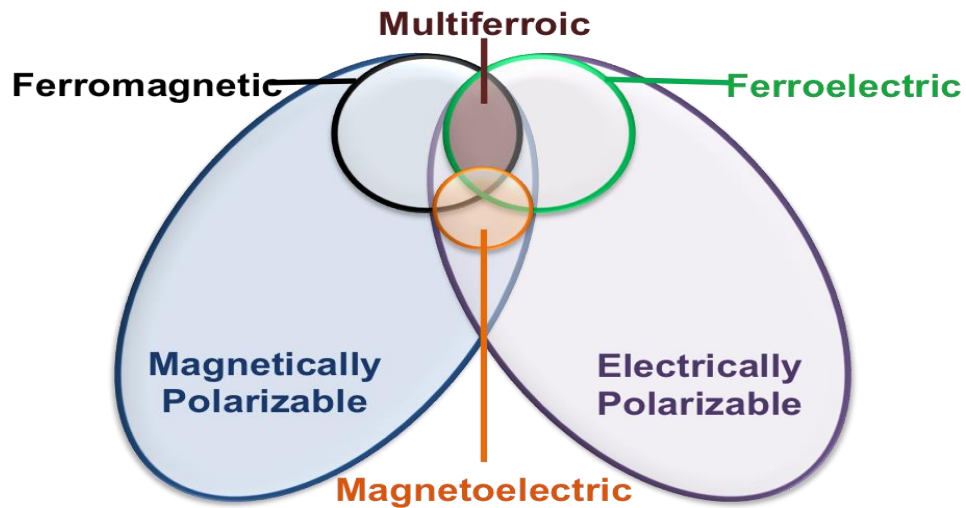


Fig.1 shows the schematic diagram of multiferroics [9]

II. MULTIFERROICS:-

The materials with the existence of different ferroic order parameters are categorized as multiferroics. The coupling between electric and magnetic order parameters develops magnetoelectricity which has been a gained a lot of attention. The fig.1 describes that magnetically polarizable materials form the superset of ferromagnetic materials and electrically polarizable materials form the superset of ferroelectric materials. The intersection of both represents the multiferroics and magnetoelectrics. All the muliferroics exhibit magnetoelectricity but vice versa is not true. For multifforicity to be exist in a material, the following order parameters are very much essential and that are described below. [10]

Primary Ferroic Order Parameters Are:-[11]

- Ferromagnetism
- Ferroelectricity
- Ferroelasticity
- Ferrotoroidicity

➤ **Ferromagnetism:-**

In Ferromagnetic materials the spins are lined up in a directions same as that of atomic level and the region is called domain and are considered as the long-range ordered material. The magnetic field are intense in the region where the spins are aligned parallel to each other. These materials have high coercive field and remnant magnetization due to which they are purposely used in various industries.

➤ **Ferroelectricity:-**

Similar to ferromagnetism, Ferroelectricity is a property of certain materials in which they possess a spontaneous electric polarization with the application of an external electric field. The high coercivity, and saturation polarization implies higher dielectric constant for which they can be used to make capacitors with tunable capacitance.

➤ **Ferroelasticity:-**

Ferroelasticity is a phenomenon in which a material exhibits spontaneous deformation with the application of strain. Ferroelastic materials display a spontaneous deformation that is stable and can be switched hysteretically by the application of applied stress. Ferroelasticity is the mechanical equivalent of ferroelectricity and ferromagnetism.

➤ **Ferrotoroidicity:-**

Ferrotoroidicity, a spontaneous alignment of magnetic vortices. The materials possess a stable and spontaneous order parameter that is taken to be the magnetization or polarization. The ferrotoroidic state differs from the other forms of ferroic order in its asymmetric behaviour.

III. PEROVSKITES:-

The perovskite oxides are appeared as one formula unit of ABO_3 and possess ideally cubic or close to cubic lattice symmetry and are termed as single perovskites. Here the central metal ion is surround by the six oxygen atoms. Due to the atomic arrangement, these perovskite oxides exhibit most prominent features such as ferroelectricity, piezoelectricity and multiferroicity etc. The ABO_3 oxide in which the net positive and negative charge centres coincide are considered as ideal perovskites. [12] But in general, these two charge centers doesn't coincide resulting a net dipole moment that generates significant ferroelectricity in the material. In some of the perovskites, ferroelectricity can coexist with forms of ferromagnetism in single phase as well as in compounds. In single phase perovskites, the multiferroicity arise due to the dissimilar metal ion. This is observed for many single perovskites like $BiFeO_3$. These are used for micromechanical actuation and non-volatile memories etc. Other application areas include tunable radio frequency devices, solid electrolytes, and solid state cooling. [13]

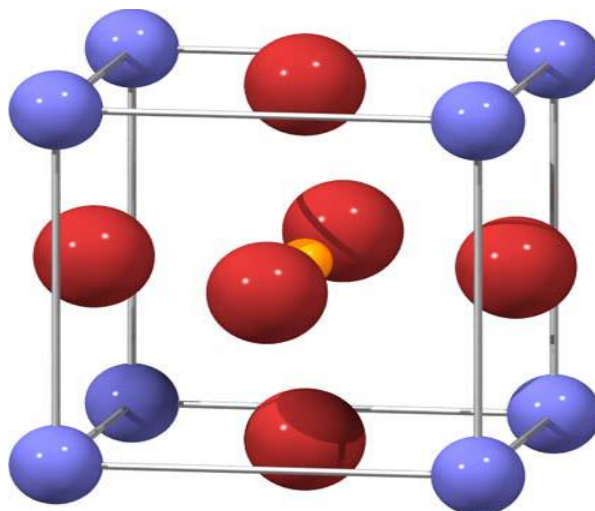


Fig.2 shows the schematic diagram a single perovskite where Blue spheres represent the A cations, yellow Spheres represent the B cation, and red spheres represent oxygen anions forming an octahedral. [13]

III.1 Double perovskite:-

Double perovskites are of the form $A_2BB'O_6$ i.e. $ABO_3 \cdot AB'O_3$. The double perovskite structure is so named because the unit cell of is repeated twice that of perovskite. It has the same architecture of 12 coordinate A sites and 6 coordinate B sites, but two cations are ordered on the B site. B ions are usually magnetic; Fe, Co, Ni, Cr or Mn [14] while B' is typically non magnetic i.e. Mo. B and B' sites are center of oxygen octahedral i.e. they are co-ordinated with six oxygen. so two types of BO_6 and $B'O_6$ sites are repeated in three directions to give the structure. They exhibit variety of optical, electric and magnetic properties. Large number of possible B, B' combinations in double perovskites lead to variety of magnetic phases i.e. ferromagnetic, antiferromagnetic, spin glass etc. Physical properties depend on chemical combination of B and B' and ionic radius and valency of A – atom. They exist in semiconductor, insulator and superconductor form. [15]

III.2 ABOUT $\text{La}_2\text{NiMnO}_6$:-

LNMO, having general structure of double perovskite ($\text{A}_2\text{BB}'\text{O}_6$) is distorted from ideal double perovskite and the amount of distortion changes as the temperature changes. [16] The structure of $\text{La}_2\text{NiMnO}_6$ is monoclinic with space group $\text{P2}_1/\text{n}$. It is a ferromagnetic insulator with Curie temperature, $T_c=280\text{K}$. In LNMO, the Ni-d states and Mn-d states suggests the oxidation states to be +2 and +4 respectively. LNMO being an insulator, the ferromagnetism in the compound is expected to be dominated by the localized superexchange type of interaction of the half-filled d-orbitals of one metal ion with the vacant d-orbital of another metal ion. [17] Hence there is hopping of interactions between effective Ni-d and Mn-d orbitals. [18] The virtual hopping of parallelly aligned spins is allowed and is favoured over antiparallel aligned spins.

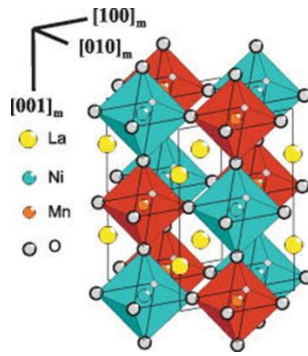


Fig.3 shows the schematic diagram of $\text{La}_2\text{NiMnO}_6$

CHAPTER 2

LITERATURE SURVEY:

1. Min zhu *et al.*,Appl.phys.Lett.100,062406(2012):

- ✓ The ground states of $\text{La}_2\text{NiMnO}_6$ and $\text{La}_2\text{CoMnO}_6$ are ferromagnetic semiconducting with alternate Ni/Mn and Co/Mn ordering along (111) direction.
- ✓ $\text{La}_2\text{NiMnO}_6$ and $\text{La}_2\text{CoMnO}_6$ are half metal with Ni/Mn or Co/Mn ordering along (001) and (110) after considering the effect of electronic correlation.

2. Shiming zhou, *et al.*,Appl.phys.Lett 91,172505(2007) :

- ✓ The magnetic properties of the double perovskites structure have been found by electron spin resonance.
- ✓ The electron spin resonance spectra reveal that a pure paramagnetism regime only exist above $T = 390\text{K}$.
- ✓ The bulk sample of LNMO is usually prepared by solid state reaction method.
- ✓ Near room temperature , superexchange interaction between N^{+2} AND Mn^{+4} are shown due to ferromagnetism of LNMO.
- ✓ The ESR spectra gives the clear evidence of the presence of short range magnetic ordering, which is consistent with the recent Raman studies.

3. H.Z.Guo, *et al.*,Physical review B 77,174423(2008):

- ✓ The Raman peaks of the LNMO thinfilms grown in the 800mTorr background O_2 are blueshifted in comparison to those of bulk LNMO, and the shift increases with decreasing film thickness, indicating the increased influence of strain.

- ✓ The scanning transmission electron microscopy results confirm that the films are epitaxial, and the interface is sharp and coherent.
- ✓ The films of double perovskites $\text{La}_2\text{CoMnO}_6$ have been grown by pulsed laser deposition under different oxygen background pressure (25-800 mTorr) condition.

4. Jun Li, et al., WILEY-VCH Verlag GmbH and co. KGAA, WEINHEIM (2005):

- ✓ The structure of $\text{La}_2\text{NiMnO}_6$ is rhombohedral at high temperature and transforms into monoclinic at low temperature.
- ✓ Single phase samples of $\text{La}_2\text{NiMnO}_6$ were prepared using conventional solid state synthetic method.
- ✓ The pure 100% monoclinic phase is at 3.5 K
- ✓ The temperature and field dependent resistivities were measured by using four probe method.

5. M.P. Singh, et al., Appl. Phys. Lett. 91, 042504 (2007):

- ✓ For the measurement of temperature dependence of dielectric constant, the frequency range is 10^{-10} to 10^5 Hz under applied magnetic fields up to 5 KOe.
- ✓ The dielectric constants (ϵ) of LCMO film was measured on a capacitor structure realized by depositing indium dots directly onto the LCMO/Nb:SrTiO₃.
- ✓ Magnetic properties of LCMO films were measured by using a superconducting quantum interference from quantum design.

6. J-Q.Yan, *et al.*, Physical Review B 68,064415(2003):

- ✓ Normalised $\text{La}_2\text{NiMnO}_6$ by solid state reaction in air.
- ✓ Synthesis by Pechini method in Ar, air and O_2 atmosphere under different thermal treatments also consistently gave $\text{O}_{6+\delta}$; the lowest of $\delta=0.05$ was attained for a single $\text{P2}_1/\text{N}$ phase.
- ✓ In this synthesis, 1.5 times the stoichiometric amount of citric acid was then added to accomplish complete chelation.

7. M.N. LLIEV, *et al.*, Applied Physics Letters 90,151914(2007):

- ✓ In the preparation of thin film, the LNMO thin film (150nm) were deposited on cubic(001) LaAlO_3 (LAO) substrates by pulsed laser deposition at oxygen pressure of 800mTorr.
- ✓ The Raman spectra were measured in backward scattering configuration with 488nm Ar^+ laser excitation using an HR640 single spectrometer.

8. Y.Q.Lin, *et al.*, Solid state comm. 149(2009)

- ✓ The ordered $\text{Ni}^{2+}\text{-O-Mn}^{4+}$ super exchange interactions give rise to the high ferromagnetic curie temperature of 280k.
- ✓ The dense $\text{La}_2\text{NiMnO}_6$ ceramics were obtained by sintering at 1723k in air for 3hr. The final pellets were 1.5mm in height and 10mm in diameter.
- ✓ The tendency of dielectric response of $\text{La}_2\text{NiMnO}_6$ ceramics is similar to that of crystalline $\text{La}_2\text{NiMnO}_6$ thin films.

9.W. Z. Yang, *et al.*, J. Appl. Phys. 111, 084106 (2012):

- ✓ Bulk $\text{La}_2\text{NiMnO}_6$ was reported to exhibit giant magneto dielectric effects at room temperature.

- ✓ $\text{La}_2\text{Ni}(\text{Mn}_{1-x}\text{Ti}_x)\text{O}_6$ ($x=0,0.2,0.4,0.6,0.8$ and 1) ceramics were prepared by solid state sintering process.
- ✓ The dielectric characteristic was measured with broad band dielectric spectrometer.

CHAPTER 3

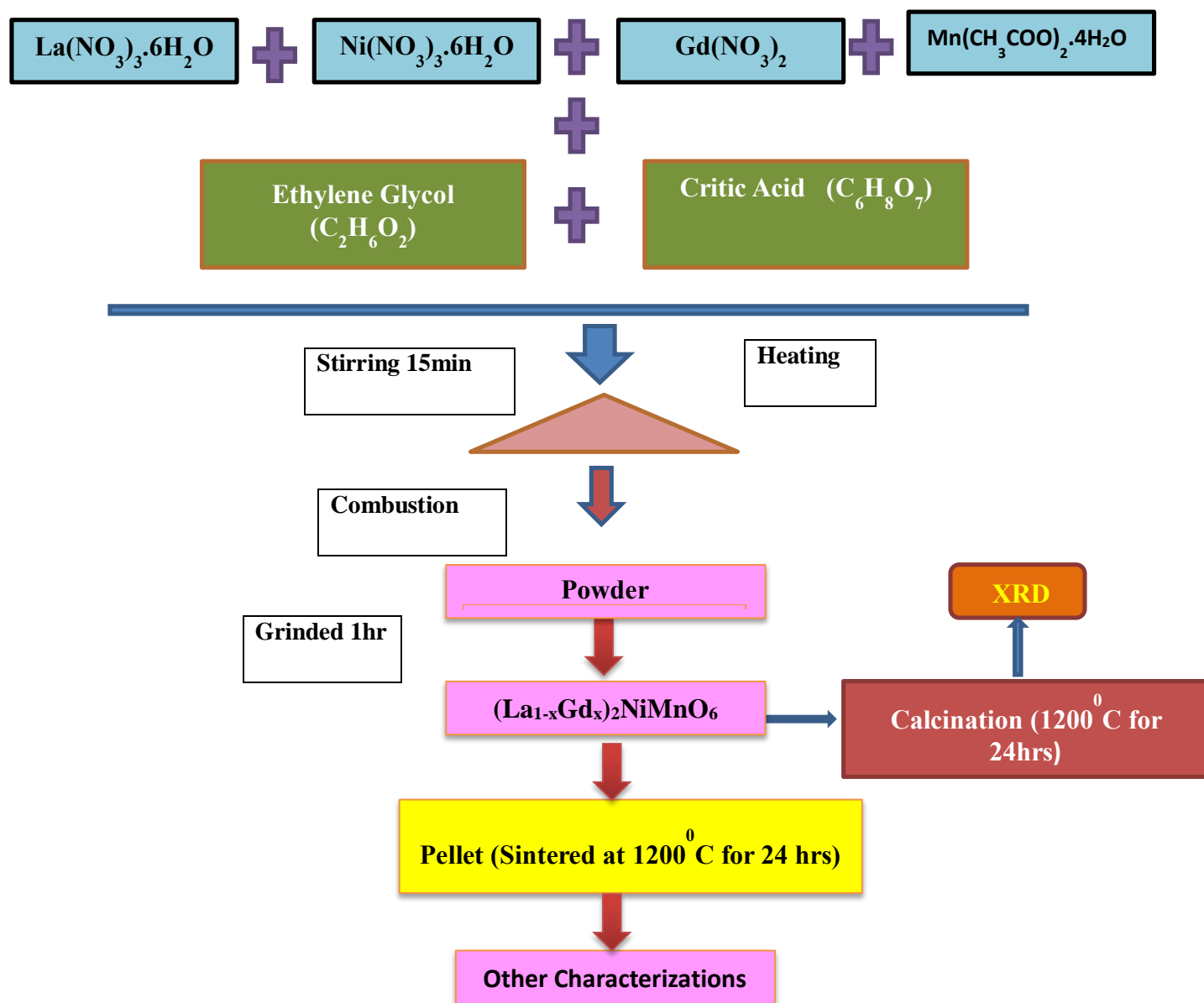
Experimental

I. Synthesis

The $(\text{La}_{1-x}\text{Gd}_x)_2\text{NiMnO}_6$ samples are prepared in sol gel combustion route. Stoichiometric amount of lanthanum nitrate $(\text{La}(\text{NO}_3)_3 \cdot 6\text{H}_2\text{O})$, nickel nitrate $(\text{Ni}(\text{NO}_3)_2 \cdot 6\text{H}_2\text{O})$, manganese acetate $(\text{Mn}(\text{CH}_3\text{COO})_2 \cdot 4\text{H}_2\text{O})$ and anhydrous Gadolinium nitrate $(\text{Gd}(\text{NO}_3)_3)$ were taken as precursors. A beaker, spatula and a piece of aluminium foil are cleaned with acetone for measurement. 1M citric acid and ethylene glycol are taken as chelating agents. Few drops of concentrated Nitric acid (HNO_3) are poured into the solution to make manganese acetate dissolved in water and to maintain the pH. An emerald green colored solution of all precursors is obtained and heated in hot plate with continuous stirring. After 2 to 3 hours, due to continuous evaporation of water, an emerald color gel at the bottom of the beaker is obtained. The gel is burnt vigorously with glows and forming a fluffy blackish powder. The collected powder from the beaker is grinded for about one hour with mortar pestle. Then from the powder sample, two to three pellets of 10mm diameter are prepared by dry pressing method with 50kg/m^2 pressure applied for two minutes. All the prepared pellets along with the remaining powder sample are calcined at 1200°C for 24 hours.

The schematic diagram is given below.

II. Flow Chart:-



CHAPTER 4

Results and Discussions:-

I. XRD measurement

The confirmation of the single phase and the crystal structure is obtained from the room temperature x-ray diffraction for $(\text{La}_{1-x}\text{Gd}_x)_2\text{NiMnO}_6$ ($x = 0, 0.1, 0.2$) powders in the 2θ range 20° to 80° with a scanning rate $3^\circ/\text{min}$. The measurement is performed in Rigaku Ultima IV system. Fig.4 shows the XRD pattern for all the samples and are well crystallized in monoclinic structure with space group $\text{P}2_1/\text{n}$ without any appearance of secondary phase. From Reitveld refinement (not shown here) the lattice parameter for the pristine sample is found to be $a=5.4548 \text{ \AA}$, $b=5.503 \text{ \AA}$, $c=7.7304 \text{ \AA}$ along with $\alpha=\gamma=90^\circ$ and $\beta=89.93^\circ$.

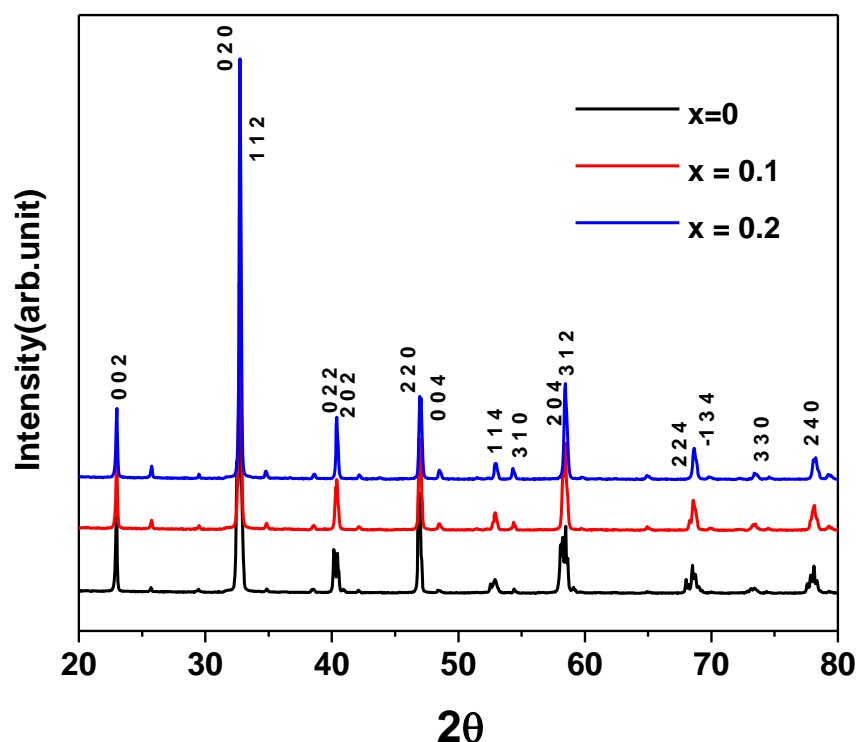


Fig. 4 shows the XRD pattern of $(\text{La}_{1-x}\text{Gd}_x)_2\text{NiMnO}_6$ ($x = 0, 0.1, 0.2$) samples .

II. DC resistivity measurement

To investigate the intrinsic electrical conduction, all the samples are subjected to the temperature dependent two probe dc resistivity (ρ) measurement as shown in fig. 5. The temperature dependent electrical transport measurements are done with the help of closed cycle refrigerator (Janis), electrometer (Keithley 6517B) and temperature controller (Lakeshore 331). It is observed that the room temperature resistivity of the samples goes on increasing with increase in the Gd concentration enhancing the insulating behavior of the pristine sample. The behavior of $x = 0$ and 0.2 is quite similar and reflects the signature of insulating sample whereas $x = 0.1$ shows a peculiar behavior where resistivity got saturated at $\sim T = 200\text{K}$. To understand the underlying physics for $x = 0.1$ it needs further study.

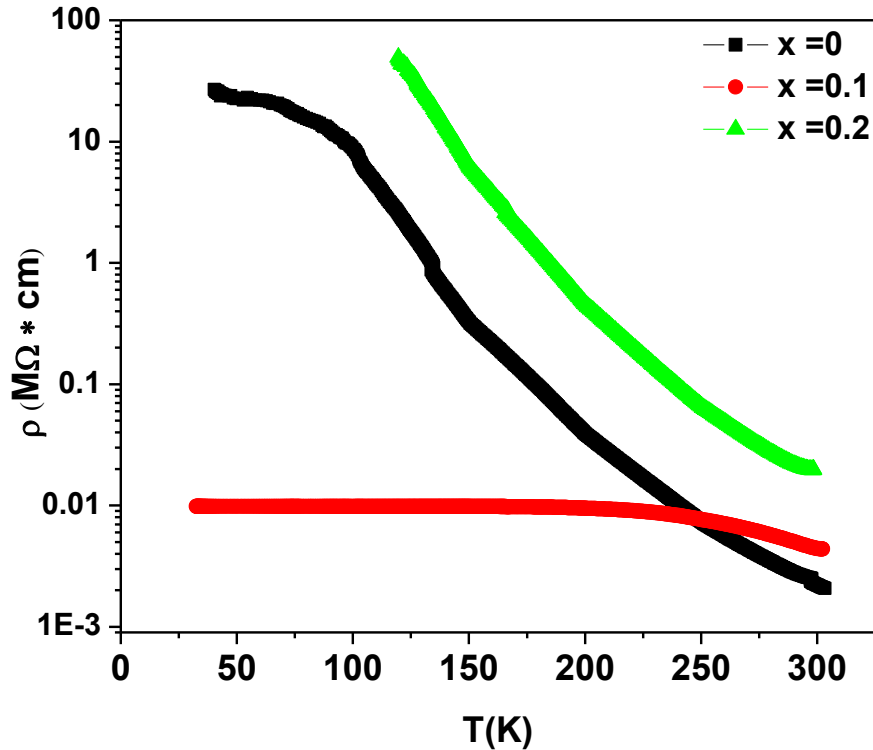


Fig.5 shows the combined plot of dc electrical resistivity measurement of $(\text{La}_{1-x}\text{Gd}_x)_2\text{NiMnO}_6$ ($x = 0, 0.1, 0.2$) samples.

The clear footprint of thermally activated behavior is observed for all the three samples. For the sake of clarity, fig. 6 shows the individual plot of $\ln\rho$ vs. $1000/T$ for $x=0, 0.1, 0.2$.

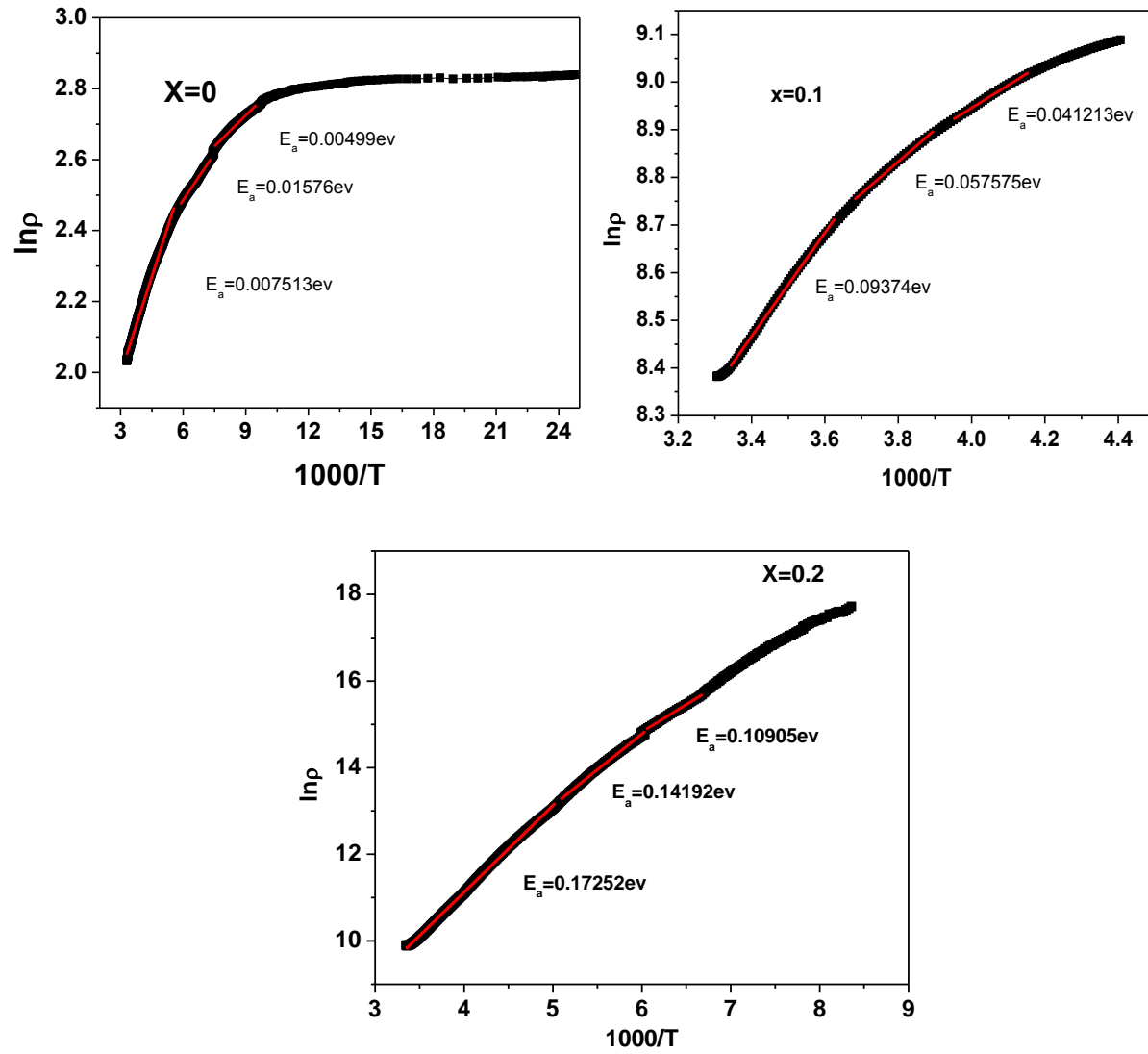


Fig.6 $\ln\rho \sim 1000/T$ plot for $(La_{1-x}Gd_x)_2NiMnO_6$ ($x= 0, 0.1, 0.2$) samples. Resistivity is showing thermally activated behavior. Red lines show the linear fit to the resistivity plot.

All the plots are fitted with the Arrhenious behavior for the confirmation of the thermally activated behavior. The Arrhenious euation can be written as:

$$\rho = \rho_0 e^{-E_a/kT}$$

Where ρ is the resisivity,

ρ_0 = pre exponential factor,

E_a = activation energy,

k = Boltzman's constant,

T = Temperature

The linear portion of fig. 6 are fitted with the above equation and the slope of that region gives the corresponding activation energy. It has been observed that for all the three samples the activation energy decreases with the increase in temperature. All the three samples shows three activation energy within the measured temperature range. In addition to this the activation energy is increasing with the increase in Gd concentration.

III. Dielectric Measurement:-

a. Temperature Variation:

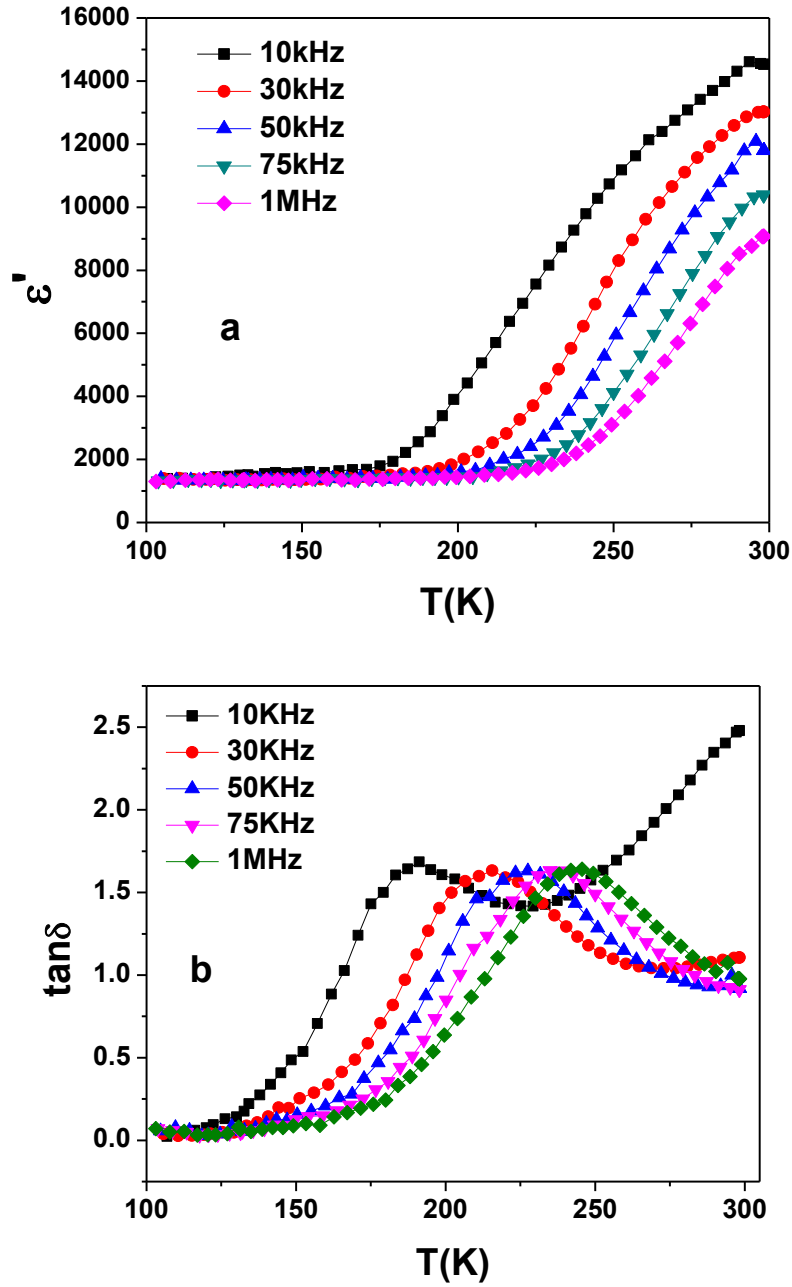
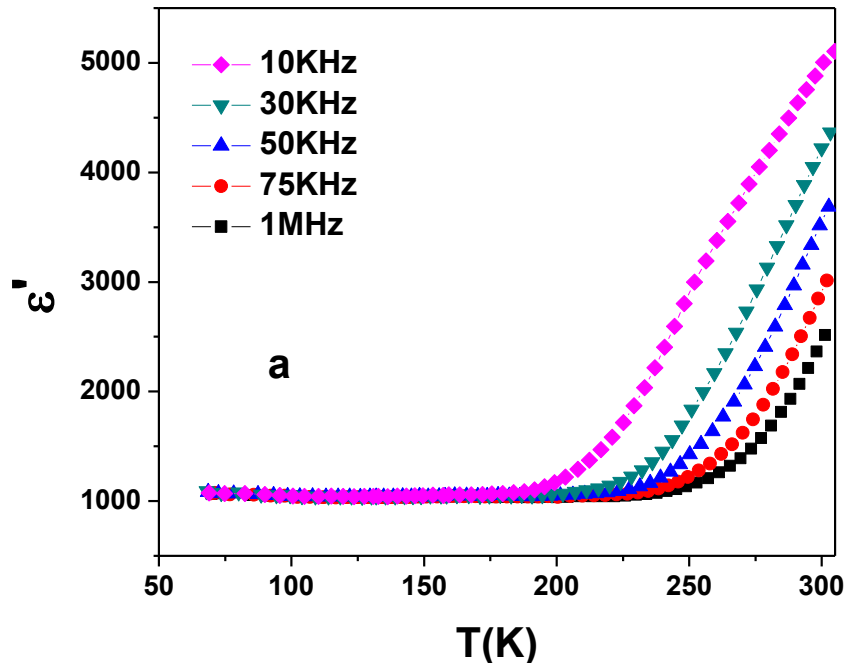


Fig.7 Low temperature behavior of ϵ' and $\tan\delta$ for $\text{La}_2\text{NiMnO}_6$

Low temperature dielectric measurement is done by Stanford SR 830 Lock in Amplifier equipped with a Closed Cycle refrigerator (CCR) and Lakeshore 331 temperature controller. The data is collected in the temperature range 300K – 50K while cooling. Fig.7, 8 and 9 show the temperature dependence of real part of dielectric permittivity (ϵ') and loss tangent ($\tan\delta$) for all three compositions. Dielectric data of LNM (Fig 7a.) show a monotonic decrease in dielectric constant with decrease in temperature up to a temperature 175K. Below 175K ϵ' value reaches its minima and doesn't show any dispersion till the lowest temperature achieved. The ϵ' plateau (300 K – 175K) show strong frequency dispersion and $\tan\delta$ (See Fig 7b.) spectra show a corresponding relaxation peak near about temperature 225K. The relaxation peak also shows strong frequency dispersion.



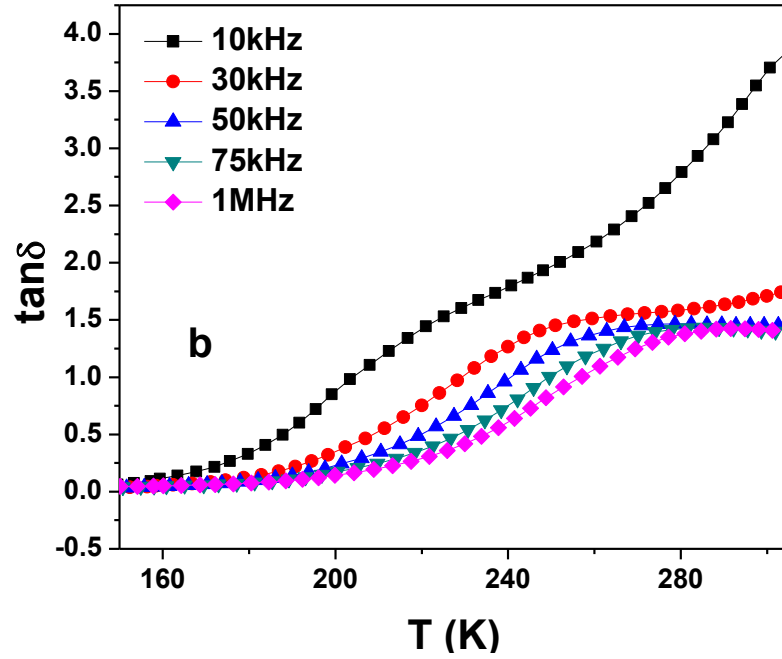


Fig.8 Low temperature behavior of ϵ' and $\tan\delta$ for $(\text{La}_{0.9}\text{Gd}_{0.1})_2\text{NiMnO}_6$

Similar behavior is observed for 10%Gd substituted sample. The ϵ' plateau (See Fig.8a) reaches at its minimum value at somehow higher temperature (200K) than that of LNM (175K). Similar frequency dispersion is also observed for this sample. The relaxation peak at 260K in loss spectra (See Fig 8b) is occurring at a higher temperature than that for LNM (225K).

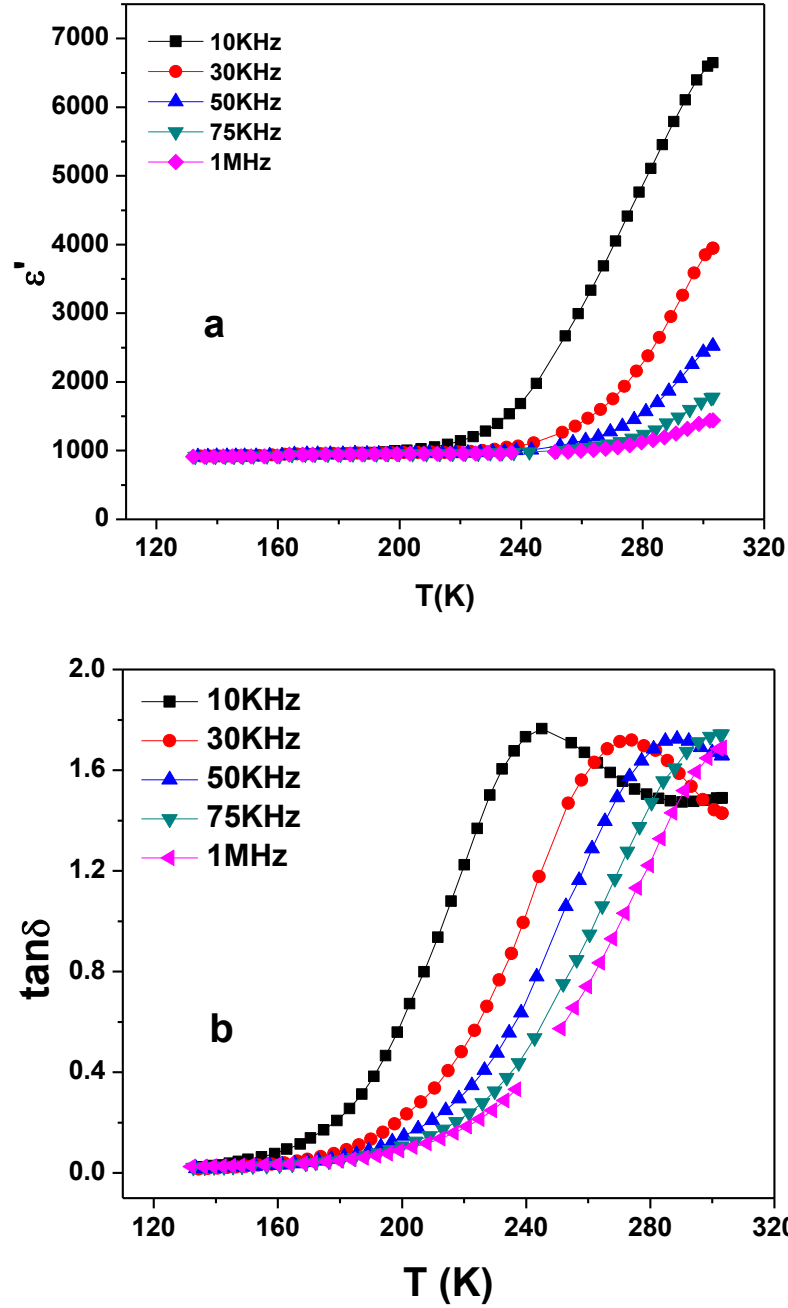


Fig.9 Low temperature behavior of ϵ' and $\tan\delta$ for $(\text{La}_{0.9}\text{Gd}_{0.2})_2\text{NiMnO}_6$

For 20% Gd substituted sample, the temperature window is narrowed again that means ϵ' value reaches at its minima at a temperature 220K (See Fig. 9a). ϵ' also show strong frequency dispersion and the loss spectra show corresponding relaxation peak around 260K (See Fig. 9b).

The relaxation peak is observed at higher temperature than all other three compositions. So with increase in Gd concentration the temperature range for the ϵ' plateau becomes narrower and the corresponding relaxation peak in loss spectra shifts to higher temperature.

b. Frequency Variation:

Room temperature dielectric loss (ϵ'') in the frequency range 100 Hz - 100 KHz is plotted in Fig.10. Loss spectra for LNM show a monotonic decrease in ϵ'' value with increase in frequency. At high frequency there is a signature of a dielectric relaxation peak. With increase in Gd- concentration dielectric loss decreases. Another important observation is that the high frequency loss peak is shifted to lower frequency with increase in Gd – concentration.

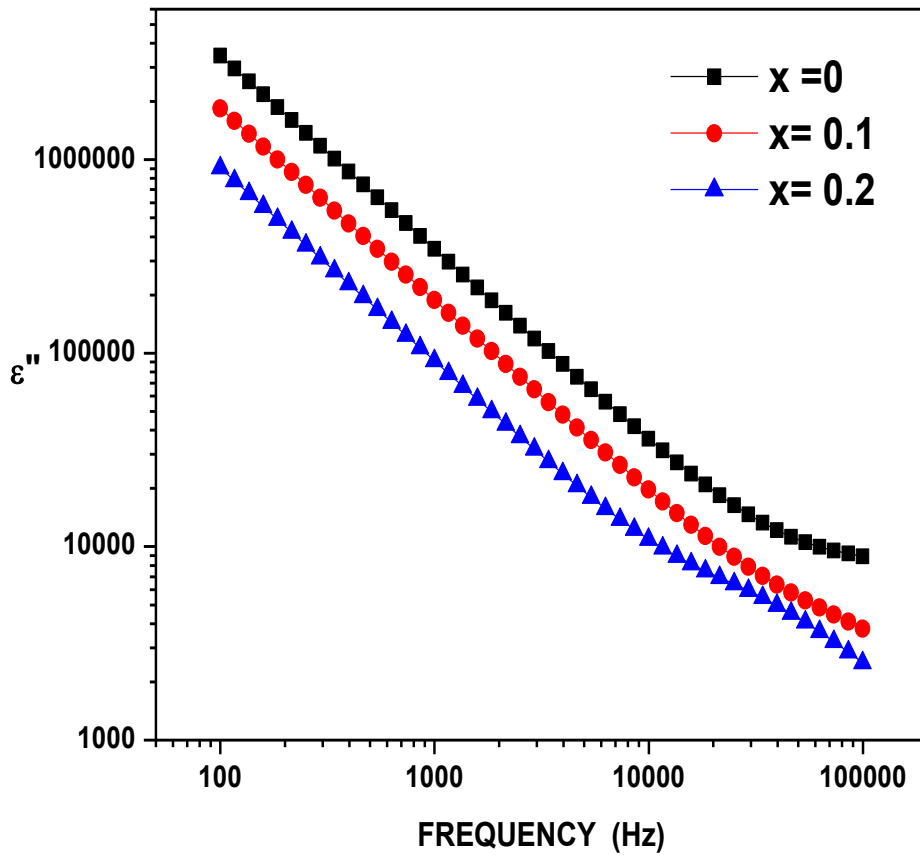


Fig.10 Room temperature ϵ'' spectra of $(\text{La}_{1-x}\text{Gd}_x)_2\text{NiMnO}_6$, where $x = 0, 0.1, 0.2$

CHAPTER 5

CONCLUSION:-

The $(\text{La}_{1-x}\text{Gd}_x)_2\text{NiMnO}_6$ samples are successfully prepared by sol-gel route. The samples are calcined at 1200°C . The X-ray diffraction for all the sample confirms the formation of single phase with monoclinic crystal structure and the space group is $\text{P}2_1/\text{n}$. The temperature dependent electrical transport measurements results the insulating behavior for all the samples. It is observed that the room temperature resistivity of the samples goes on increasing with increase in the Gd concentration enhancing the insulating behavior of the pristine sample. The clear footprint of thermally activated behavior is observed for all the three samples and is confirmed through the Arrhenius equation. The activation energy is found to decrease with increase with temperature and in addition to this it increases with increase in Gd concentration. The temperature dependence of real part of dielectric permittivity (ϵ') and loss tangent ($\tan\delta$) for all three compositions results the shifting of non-dispersive region of ϵ' and relaxation peak of $\tan\delta$ towards the higher temperature with increase in Gd concentration. Room temperature dielectric loss (ϵ'') spectra shows a monotonic decrease in ϵ'' value with increase in frequency. One of the important observation is that the high frequency loss peak is shifted to lower frequency with increase in Gd – concentration.

REFERENCES:-

1. <http://www2.rowland.harvard.edu/book/oxides-research-group>
2. http://en.wikipedia.org/wiki/High-temperature_superconductivity
3. <http://phys.org/tags/high+temperature+superconductors/>
4. <http://en.wikipedia.org/wiki/Ferroelectricity>
5. <http://www.news.cornell.edu/stories/2012/04/ferroelectric-oxides-do-twist>
6. Lee et. al., *J. Eur. Ceram. Soc.* **32** 3971 (2012)
7. <http://www.ak-tremel.chemie.uni-mainz.de/220.php>
8. Rao et. al., *J. Phys. Chem. Lett.* **3**, 2237 (2012)
9. Wu et. al., *Nanoscale Res. Lett.* **8**, 207 (2013)
10. Prellier et. al., *J.Phys: Condens.Matter* **17**, R803 (2005)
11. ethesis.nitrkl.ac.in/1704/1/final_report_achyuta.pdf
12. <http://winntbg.bg.agh.edu.pl/rozprawy2/10056/full10056.pdf>
13. <http://abulafia.mt.ic.ac.uk/publications/theses/levy/Chapter3.pdf>
14. Singh et. al., *J. Appl. Phys.* **107**, 09D917 (2010)
15. Zhu et. al., *Appl.phys.Lett.* **100**, 062406 (2012)
16. Zhou, et. al., *Appl. phys. Lett.* **91**, 172505 (2007)
17. GuO, et. al., *Phys. Rev. B* **77**, 174423 (2008)

18. Singh et. al., *Appl. Phys. Lett.* **91**, 042504 (2007)
19. Yan et. al., *Phys. Rev. B* **68**, 064415 (2003)
20. Lliev et. al., *Appl. Phys. Lett.* **90**, 151914 (2007)
21. Lin, et. al., *Solid state comm.* **149**, 1646 (2009)
22. Yang, et. al., *J. Appl. Phys.* **111**, 084106 (2012)
23. Scott et. al., *Nat. Rev.* **442**, 759 (2009)
24. Jian et. al., *Chin. Sci. Bull.* **53**, 2097 (2008)
25. <http://fptl.ru/biblioteka/spravo4niki/dean.pdf>
26. Sowmya et. al., *Handbook of Advanced Ceramics: Processing and their applications*, **2**.
Elsevier Academic Press (2009)
27. Lee et. al., *Phys. Rev. B* **78**, 100101 (2008)